

Article

Preparation and Preliminary Dielectric Characterization of Structured C₆₀-Thiol-Ene Polymer Nanocomposites Assembled Using the Thiol-Ene Click Reaction

Hanaa M. Ahmed ^{1,5}, Amber D. Windham ¹, Maryam M. Al-Ejji ², Noora H. Al-Qahtani ²,
Mohammad K. Hassan ², Kenneth A. Mauritz ³, Randy K. Buchanan ⁴ and J. Paige Buchanan ^{1,*}

Received: 30 September 2015 ; Accepted: 12 November 2015 ; Published: 18 November 2015

Academic Editor: Biqiong Chen

¹ Department of Chemistry and Biochemistry, University of Southern Mississippi, 118 College Drive, Hattiesburg, MS 39406, USA; Hanaa.ahmed76@gmail.com (H.M.A.); amber.gresham@eagles.usm.edu (A.D.W.)

² Center for Advanced Materials, Qatar University, Doha P.O. Box 2713, Qatar; maryam.alejji@qu.edu.qa (M.M.A.-E.); noora.alqahtani@qu.edu.qa (N.H.A.-Q.); mohamed.hassan@qu.edu.qa (M.K.H.)

³ School of Polymers and High Performance Materials, University of Southern Mississippi, Hattiesburg, MS 39406, USA; kenneth.mauritz@usm.edu

⁴ U.S. Army Engineer Research and Development Center, Information Technology Laboratory, Institute for Systems Engineering Research, 3909 Halls Ferry Road, Vicksburg, MS 39180, USA; Randy.K.Buchanan@erdc.dren.mil

⁵ Faculty of Engineering, Benha University, Shoubra, Benha 13 512, Egypt

* Correspondence: paige.buchanan@usm.edu; Tel.: +1-601-266-4083; Fax: +1-601-266-6075

Abstract: Fullerene-containing materials have the ability to store and release electrical energy. Therefore, fullerenes may ultimately find use in high-voltage equipment devices or as super capacitors for high electric energy storage due to this ease of manipulating their excellent dielectric properties and their high volume resistivity. A series of structured fullerene (C₆₀) polymer nanocomposites were assembled using the thiol-ene click reaction, between alkyl thiols and allyl functionalized C₆₀ derivatives. The resulting high-density C₆₀-urethane-thiol-ene (C₆₀-Thiol-Ene) networks possessed excellent mechanical properties. These novel networks were characterized using standard techniques, including infrared spectroscopy (FTIR), differential scanning calorimetry (DSC), dynamic mechanical analysis (DMA), and thermal gravimetric analysis (TGA). The dielectric spectra for the prepared samples were determined over a broad frequency range at room temperature using a broadband dielectric spectrometer and a semiconductor characterization system. The changes in thermo-mechanical and electrical properties of these novel fullerene-thiol-ene composite films were measured as a function of the C₆₀ content, and samples characterized by high dielectric permittivity and low dielectric loss were produced. In this process, variations in chemical composition of the networks were correlated to performance characteristics.

Keywords: dielectric properties; fullerenol; thiol-ene; nanocomposites

1. Introduction

C₆₀ fullerene-containing polymers are receiving increased attention due to their remarkable properties and anticipated applications. Recent reviews describe the inclusion of C₆₀ into main-chain, side-chain, cross-linked, and star-shaped polymer configurations [1,2]. C₆₀'s three dimensional structure yields a unique versatility in constructing high-molecular weight polymer architectures. An

interesting feature of these C₆₀-polymer nanocomposites lies in the possibility of tuning the physical properties and therefore resulting potential applications of the composite through modification of the chemical linkages among the matrix constituents. Demonstrating this versatility, there are interesting reports of C₆₀'s incorporation into polymer composites as blends to create photo-active and stimuli-responsive coatings [3], C₆₀-derivative-styrene blends [4] and covalent C₆₀-styrene copolymers [5], C₆₀-polyurethanes via reaction of the hydroxylated C₆₀ [6,7], and composites prepared in polyethylene and polyamide matrix materials [8,9].

In addition to the standard techniques to measure thermal and mechanical performance of polymer composite materials, the lesser-used method of dielectric spectroscopy is employed to characterize molecular dynamics and electrical polarizability of the networks [10,11]. The dielectric response results from the interaction of dipoles or polarizable elements with an oscillating applied electric field (f) at a given temperature. The essential quantity is the complex dielectric permittivity which is given by Equation (1),

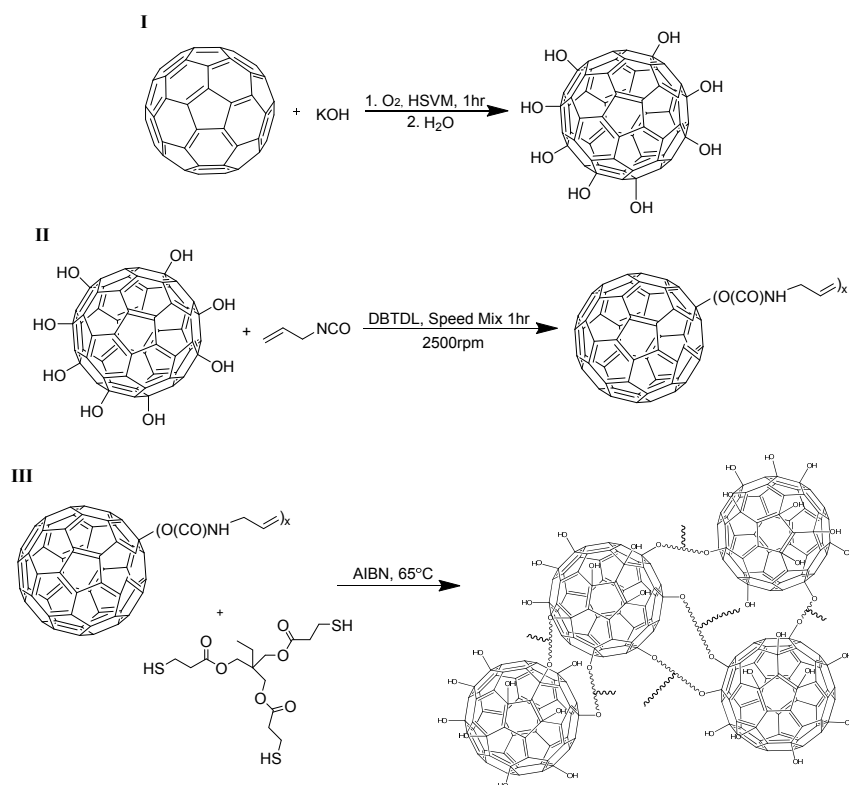
$$\varepsilon^*(\omega) = \varepsilon'(\omega) - i\varepsilon''(\omega) \quad (1)$$

where ω is the angular frequency = $2\pi f$ and $i = \sqrt{-1}$. ε' is referred to as the real permittivity and describes the material polarizability due to dipole reorientation, deformation of delocalized electron distributions, or interfacial polarization internal to the sample or at the sample/electrode interface. ε'' , the imaginary, or loss permittivity, is proportional to the energy dissipated per cycle during any of these processes, termed "relaxations". Modern broadband dielectric spectroscopy (BDS) techniques allow the analysis of samples across a wide frequency window (10^{-3} to 10^6 Hz) and is therefore a very powerful tool for probing molecular dynamics of polymers *versus* temperature [10].

Recently our group reported the preparation and characterization of a series of fullerene (C₆₀ and Sc₃N@C₈₀) polymer nanocomposites built up from a hydroxylated fullerene core, which was crosslinked with a diisocyanate elastomer polyether-based oligomer [7]. Multiple relaxations were characterized from the dielectric analysis of this system and assigned to the glass transition temperature (T_g), crankshaft motions of the ether segments, reorientation of the hydroxylated fullerene cages, and other local motions. Overall these fullerene-polymer networks could be rendered quite polarizable, but were complicated by a rather challenging synthetic strategy. Most recently our group has focused on efforts to increase the loading capacity of fullerene-polymer dielectric networks which, in turn, is expected to increase the dielectric permittivity while maintaining the desired low dielectric loss. The incorporation of C₆₀ and other fullerenes is notoriously hampered by the poor processing of fullerenes. Using our hydroxylated C₆₀ fullerene as the core structure, we have successfully implemented the "thiol-ene" click reaction to prepare a unique series of nanocomposites of high C₆₀ loading. Herein we report the synthesis and essential characterization of C₆₀-urethane-thiol-ene (C₆₀-Thiol-Ene) networks, thermal stability, mechanical, and dielectric properties.

2. Results and Discussion

The general synthesis route for the preparation of the fullerene-polymer networks, described as C₆₀-Thiol-Ene, is provided in Scheme 1. In this method, there is a sequential buildup of the network from the reaction of hydroxylated fullerene with allyl isocyanate to produce a reactive "ene" monomer and its subsequent reaction with an alkyl "thiol" in the prototypical thiol-ene reaction. There are a number of excellent reviews of the thiol-ene click reaction [12–14]. The thiol-ene reaction is based on a free-radical, step-growth polymerization mechanism. In general, the thiol-ene reaction's selectivity, high monomer conversions, insensitivity to molecular oxygen, and few competing reactions are many of the reasons for the recent popularity. A large number of commercially available thiols and enes permits the tailoring of polymer network properties for a variety of applications, and the attractive polymerization rates and uniform polymer networks produced make the thiol-ene matrix an ideal choice for polymer-particle composites [12,13,15].



Scheme 1. Preparation of C_{60} -Thiol-Ene Network.

The hydroxylation of C_{60} and was performed as previously reported by our group to yield an average of 29 OH groups, $C_{60}(\text{OH})_{29}$, with additional characterization provided in supplementary material [7]. Using anhydrous conditions, allyl isocyanate was combined under high shear to $C_{60}(\text{OH})_{29}$ in various ratios (2:1, 1:1, and 1:2 functional group equivalents) to yield a series of composites with increasing C_{60} content in the matrix, Table 1. This ene-functionalized C_{60} monomer was combined with the thiol monomer TMPMP and thermal initiator, thereby creating 9, 15, and 27 wt % C_{60} polymer composites, respectively. Following thermal cure brown/black, transparent composites were produced, which were easily removed from the Teflon mold and characterized. Films were sonicated briefly in MeOH to quench any residual isocyanate groups that were not captured by either SH and OH functional groups, particularly important for the 9- C_{60} -TE, where an excess of NCO to OH is added initially. At all times a 1:1 stoichiometric ratio of thiol to ene functional groups is maintained. It is noted that there are expected differences in the resulting networks from the combination of monomers chosen, specifically 9- C_{60} -TE may have a small fraction of residual urethane, thiourethane, or ene ends. Sample 15- C_{60} -TE will represent the ideal network composition from a chemical composition perspective, and 27- C_{60} -TE will possess a large fraction of unreacted carbinol groups in the resulting network. However, gel fractions of all samples are considered high, indicating well-formed networks. The contribution of these residuals is considered in drawing conclusions in the characterization of the networks.

Table 1. Compositions of prepared C_{60} -containing thiol-ene films.

Sample ID	NCO Equiv.	OH Equiv.	SH Equiv.	Wt % C_{60} *
9- C_{60} -TE	2	1	2	9
15- C_{60} -TE	1	1	1	15
27- C_{60} -TE	1	2	1	27

* wt % C_{60} was calculated from the mass of $C_{60}(\text{OH})_{29}$ in each sample in relation to the total mass of all nonvolatile film constituents, expressed as a percent.

Networks were characterized using common techniques, including gel fraction, infrared spectroscopy (FTIR), thermogravimetric analysis (TGA), differential scanning calorimetry (DSC), and dynamic mechanical analysis (DMA). A summary of the critical values are reported in Table 2. All monomer combinations produced networks characterized by high gel fractions, IR spectrums consistent with the composition, and thermal degradation onset temperatures of approximately 200 °C (IR and TGA plots included in supplementary material). DSC plots are provided in Figure 1, and illustrate the effect of varying the network chemical composition. All samples yield well-defined transitions; however, it is the ideal network 15-C₆₀-TE which is most characteristic of thiol-ene networks in appearance. This sample possesses the dip after the thermal step transition which has been attributed to the enthalpic relaxation of the thiol-ene network and has been studied extensively by our group and others [12,16].

Table 2. Characterization of C₆₀-TE films.

ID	Gel %	T _g (°C) by DSC	T _g (°C) by DMA	DMA Tan δ Width at ½ Height (°C)	Tan δ Peak Height
9-C ₆₀ -TE	88	−0.7	26.3	31	0.84
15-C ₆₀ -TE	94	−1.1	17.7	26	0.70
27-C ₆₀ -TE	100	−12.9	4.7	19	0.76

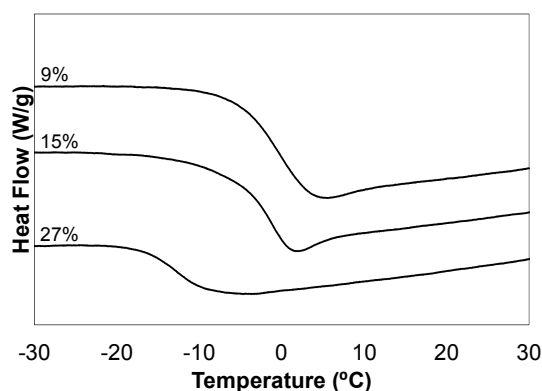


Figure 1. DSC analysis of the C₆₀-thiol-ene network film series, C₆₀ wt % in composite film noted.

Dynamic storage modulus (E') and loss tangent, $\tan \delta = E'' \cdot (\text{loss modulus})/E'$ versus temperature curves for C₆₀-thiol-ene networks are provided in Figure 2. The storage modulus curves show a glassy material at low temperatures and a rubbery material at high temperatures with a glass transition at approximately 0 °C that is associated with the onset of long-range chain segmental mobility of the thiol-ene network. The trend in the rubbery state modulus increases in the series as the C₆₀ content increases, as expected. This trend for the gel % and the rubbery state modulus also reflect the variation in crosslink density among the samples having different composition. All show a subtle peak in the temperature range of −90 to −50 °C which is associated with the crankshaft motions of the methylene sequences in the soft segments of the thiol-ene networks [7,17,18].

The peak maximum in the $\tan \delta$ plots, increasing from 26.3 to 4.7 °C, correlates to the increasing C₆₀ content of the network and represents the most active region of the glass transition at T_g. T_gs obtained by DMA measurements are reported in Table 1 along with those obtained by DSC. Regardless of the analysis method used, the T_g decreases systematically with the increase in the C₆₀%. This behavior suggests that as the concentration of C₆₀(OH)₂₉ increases in the network in relationship to the number of fullerene crosslinks, an increase in network free volume, and fullerene mobility results, thus leading to a decrease in the observed T_g. A similar trend was observed by Lu *et al.* [8] in their study of benzylaminofullerene (BAF)-polyethylene composites as a function of the BAF loading. Moreover, the maximum of the $\tan \delta$ fluctuates, with the ideal network having the lowest maximum. The presence of incomplete networks or dangling ends may lead to the increased

dampening presented by the non-ideal network samples. It is also important to notice the decreasing width of the $\tan \delta$ plots in the series, which suggest a refining of the network structure as the C_{60} fullerene concentration is increased. The initial excess of NCO to OH functional groups in synthesis would lead to a less uniform network, where a small number of fullerene urethane network bonds are likely replaced by thiourethane linkages. Finally, differences in T_g values deduced from the DMA and DSC measurements for the same samples would result from the inherent differences between the two techniques and also due to using different heating ramp rates in both experiments (2 °C/min in the DMA versus 5 °C/min for the DSC).

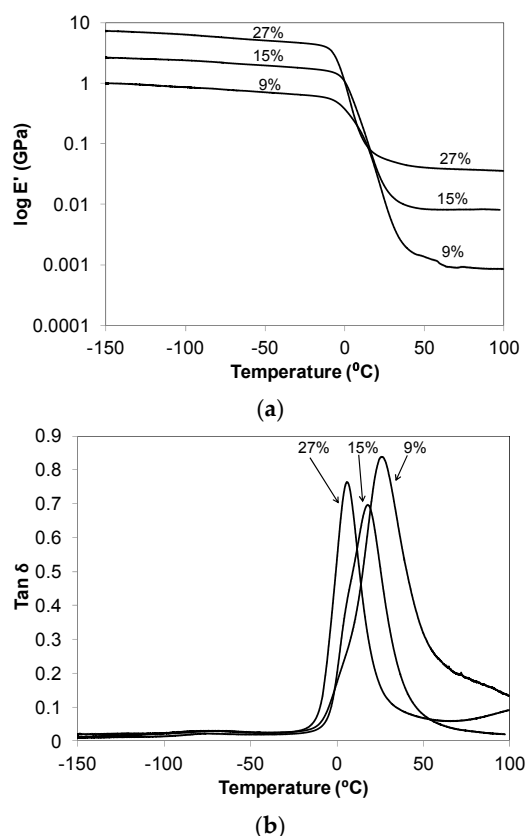


Figure 2. (a) Dynamic storage modulus (E'); and (b) loss tangent ($\tan \delta$) for the C_{60} -thiol-ene network film series, C_{60} wt % in composite film noted.

Figure 3 demonstrates the frequency dependences of the dielectric permittivity storage (ϵ') and loss (ϵ''), respectively, for networks at room temperature. These spectra were measured using a Novocontrol GmbH Concept 80 broadband dielectric spectrometer. ϵ' decreases with increasing frequency (f) and the curves are displaced upward with increasing fullerene loading. The decrease in ϵ' with increasing f is a consequence of the fact that the time scale during which the electric field is applied in one direction; that is, one-half the period of oscillation = $1/2f$, decreases with increasing frequency [7]. In essence, faster motions associated with polarizability have less time to be sampled. Increasing the C_{60} % serves to increase the polarizable network component. Additionally, at high fullerene loading, ϵ' would increase due to higher polarizability arising from the increased number of unreacted –OH groups in the composite. Other reports have suggested that as fullerene concentration increases, the dielectric permittivity of the resultant composite films may decrease due to restriction on polymer chain motions posed by these structures, specifically polyimides containing C_{60} and C_{70} fullerenes [19] and C_{60} /poly(dimethylsiloxane) [20].

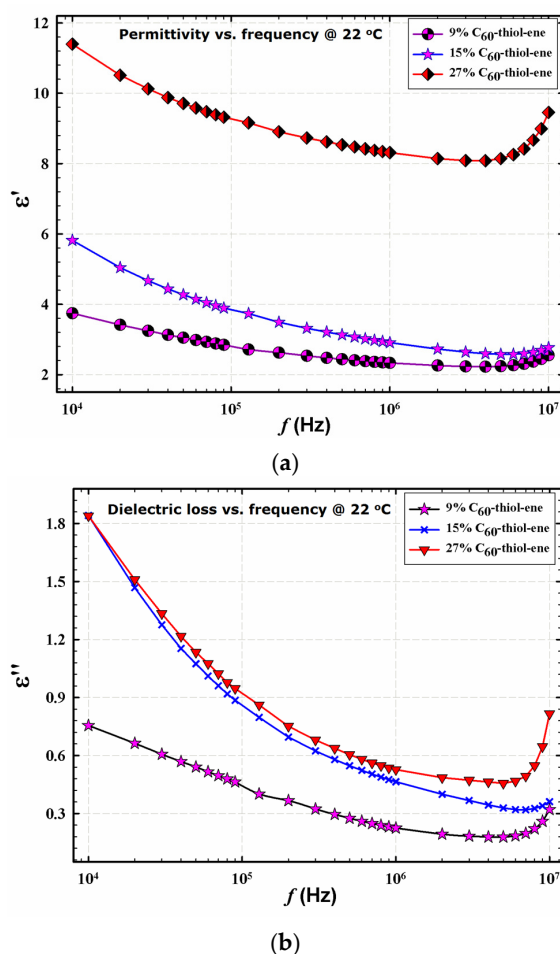


Figure 3. Dielectric permittivity storage (a); and loss (b) of films having different composition at 22 °C; C₆₀ % noted in legend.

ϵ' and ϵ'' were also determined for the prepared thiol-ene networks using an alternate test assembly comprised of a Keithley 4200-SCS (Cleveland, OH, USA) instrument and custom electrode assembly, Figure 4. The details of this assembly are reported elsewhere [7]. When compared to the results obtained using the Novocontrol broadband dielectric spectrometer shown in Figure 3, excellent correlation exists within the same frequency range. As before, both ϵ' and ϵ'' increase with increasing C₆₀ loading. The initial drop in ϵ' and ϵ'' values with increasing frequency are because at higher frequencies the dipoles do not have enough time to follow the alteration of the applied electric field. The increase in ϵ' with frequency after 7 MHz for the 27% C₆₀-thiol-ene sample might be due to a more complex polarization mechanism rather than dipole polarization. The most interesting observation in these plots is the higher values of ϵ' over ϵ'' , supporting that fullerene-containing materials such as those reported herein may prove desirable for electronic and electric systems, such as in energy storage media [21,22]. Since the maximum electrical energy storage capacity (U_{\max}) of a linear dielectric material is given by $U_{\max} = \epsilon' \cdot E_b^2 / 2$ where E_b is the dielectric breakdown strength (DBS), both large ϵ' and high DBS are required for large electric energy storage [22]. Consequently, incorporating materials with large ϵ' within polymeric matrices of high DBS and possessing excellent mechanical properties may lead to a large energy storage dielectric material. Another indicator regarding future potential of these nanocomposites as energy storage systems can be deduced from the fact that values of the ϵ' and ϵ'' can be tuned via variation of the fullerene loading. Using the laboratory methods employed herein, our group was able to produce films of high dielectric

response and low loss employing only hydroxylated C_{60} as the polarizable group using a simple synthetic strategy.

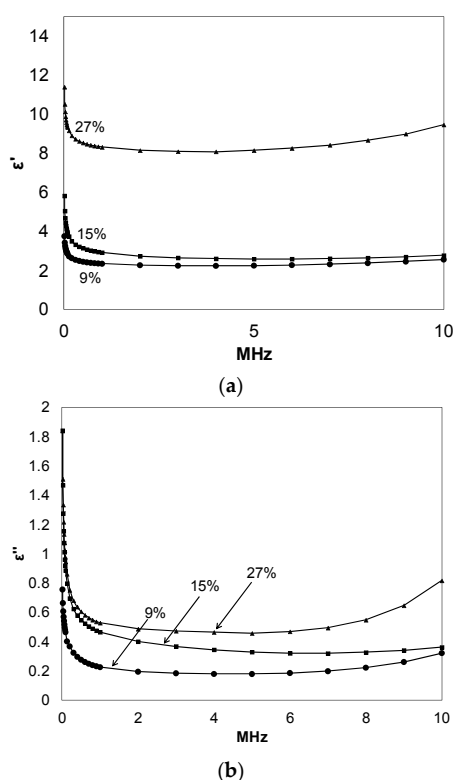


Figure 4. Dielectric permittivity storage (a); and loss (b) of films having different composition at room temperature, as measured by the semiconductor characterization system (SCS); C_{60} % noted on plots.

3. Experimental Section

3.1. Materials

The following materials were used without further purification: C_{60} fullerene (MER, 99+%, Tuscon, AZ, USA), potassium hydroxide (Sigma-Aldrich, 85+%, St. Louis, MO, USA), Sephadex G-25 (Sigma-Aldrich, 20–80 μm bead size, St. Louis, MO, USA), allyl isocyanate (Sigma-Aldrich, 98%, St. Louis, MO, USA), dibutyltin dilaurate (DBTDL, Aldrich, 95%, St. Louis, MO, USA), trimethylolpropane tris-3-mercaptopropionate (TMPMP, Sigma-Aldrich, $\geq 95\%$, St. Louis, MO, USA), pentaerythritol allyl ether (APE, Sigma-Aldrich, 70%; remaining 30% monoene, St. Louis, MO, USA), and azobisisobutyronitrile (AIBN, Sigma-Aldrich, 98%, St. Louis, MO, USA). Chloroform (Sigma-Aldrich, 99+%, St. Louis, MO, USA) was dried over 4 Å molecular sieves prior to use.

3.2. Preparation of Hydroxylated $C_{60}(\text{OH})_x$ and C_{60} -Thiol-Ene Films

The hydroxylation of C_{60} and was performed and characterized as previously reported [7]. In general, C_{60} fullerenes and KOH were combined (1:25 molar equiv.) under high-speed vibrational milling conditions using a Spex mixer/miller 8000. The resulting brown solid was dissolved in water, purified by means of Sephadex G-25 size exclusion column chromatography, concentrated, and precipitated in MeOH. Solids were collected by filtration through 0.2 μm PTFE membrane and dried under vacuum at 50 °C. The purified hydroxylated fullerenes were characterized by FT-IR spectroscopy and thermal gravimetric analysis (TGA). The dry, purified hydroxylated C_{60} was determined to have the average molecular formula $C_{60}(\text{OH})_{29}$.

Allyl isocyanate (NCO and ene) and dry C₆₀(OH)₂₉ were combined at 2:1, 1:1, or 1:2 NCO/OH equivalence, where mass of C₆₀(OH)₂₉ was divided by total mass of nonvolatile film constituents and expressed as a percent, yielding 9, 15, and 27 wt % C₆₀ films, respectively. The reaction was mixed under high shear conditions at 2500 rpm using a Speed Mixer DAC 150 FVZ-K for one hour, with the addition of DBTDL catalyst occurring after several minutes. TMPMP (SH) in dry chloroform (1 mL) was combined with the resulting ene-functionalized fullerene (1:1 SH/ene) followed by AIBN (2 wt %), with 5 min of high shear after each sequential addition. Transfers to and from reaction vessel were performed in N₂ environment. Solvent was removed under reduced pressure and the reaction mixture was transferred to a PTFE evaporating dish for thermal curing at 65 °C. The resulting film was sonicated briefly in MeOH to quench any residual reactive NCO groups, then dried at 50 °C under reduced pressure.

3.3. FT-IR and Gel Fraction

The infrared spectra of the prepared samples were recorded in the wavenumber range of 400–4000 cm⁻¹ using a Nicolet Nexus 470 FT-IR spectrometer (Madison, WI, USA). Gel fractions of prepared films were obtained by dissolving a known mass of film in chloroform, resting the sample for 24 h at room temperature, and recovering the insoluble mass fraction, followed by residual solvent evaporation under reduced pressure. The gel fraction is the final mass after extraction over the initial mass, expressed as a percent.

3.4. Thermal Gravimetric Analysis (TGA)

Thermogravimetric analysis (TGA) was used to evaluate the thermal stability of C₆₀(OH)_x for the estimation of –OH functionalities attached to the C₆₀ cage and also to evaluate the stability of the prepared fullerene-TE networks, methods as previously reported [7]. Using a TA instruments Q5000, samples were analyzed in platinum pans over the temperature range of 25–1000 °C under nitrogen and using a high-resolution heating rate of 10 °C/min. The number of hydroxyl groups attached to the fullerene cage was estimated by Equation (2):

$$\frac{\text{Formula Mass C}_{60}}{\% \text{ weight } > 570 \text{ }^{\circ}\text{C}} \times \frac{\% \text{ weight } 150 - 570 \text{ }^{\circ}\text{C}}{\text{Formula Mass} - \text{OH}} \quad (2)$$

where loss of hydroxyl addends occurs from 150 to 570 °C and the degradation of the C₆₀ cage begins at >570 °C. For fullerene-TE networks, the thermal degradation onset temperature was reported as the temperature corresponding to 10% mass loss.

3.5. Differential Scanning Calorimetry (DSC)

TA instruments modulated differential scanning calorimetry (DSC) Q2000 instrument was used to determine the glass transition temperature of fullerene-TE films over the temperature range of –50 to 150 °C in a heat/cool/heat cycle at 5 °C/min under nitrogen. T_g information was obtained from the second heat cycle.

3.6. Dielectric Measurements

Dielectric measurements on C₆₀-thiol-ene composites were performed using a Novocontrol GmbH Concept 80 broadband dielectric spectrometer, and data were collected over the frequency range 0.1 Hz–3 MHz at fixed temperatures in the range of –150 to 180 °C. The temperature stability of the instrument was within ±0.2 °C. Samples were kept in a humidity control chamber (Model 503-20, Electro-tech Systems, Inc., Glenside, PA, USA) with RH < 0.5% at room temperature for more than one week prior to analysis. Sample discs of 2 cm diameter that were covered with two very clean aluminum sheets on both sides were sandwiched between two gold-coated copper electrodes of 2 cm diameter and transferred to the instrument for data collection.

Dielectric properties were also measured using a Keithley 4200 semiconductor characterization system (SCS) connected to a custom designed parallel plate electrode assembly as previously reported. Two types of permittivity tests were performed with this assembly. The first test measured capacitance at frequencies spanning a range from 10 kHz to 10 MHz in graduated logarithmic steps with 0 VDC (volts dc) bias. For the second test, the DC offset voltage was swept from -30 to $+30$ VDC in 1 VDC steps at a constant frequency. Both tests calculated permittivity by measuring the root mean squared (rms) current at the given frequency and rms voltage. All tests were performed at room temperature ($22\text{ }^{\circ}\text{C}$) under controlled humidity. The standard equations for parallel plate capacitor geometry were used to calculate permittivity from the measured capacitance.

3.7. Dynamic Mechanical Analysis (DMA)

The dynamic storage modulus (E') as well as $\tan \delta = E''/E'$ were measured using a DMA Thermal Analysis Q800 instrument. All samples were run in tensile mode with a frequency of 1 Hz and amplitude of $15\text{ }\mu\text{m}$. The experiments were performed over the temperature range -150 to $100\text{ }^{\circ}\text{C}$ at a heating rate of $2\text{ }^{\circ}\text{C}/\text{min}$.

4. Conclusions

Alkyl thiols and ene-functionalized C_{60} fullerene were thermally polymerized to form C_{60} fullerene-thiol-ene networks. Physical and electrical properties of these networks were studied as a function of the C_{60} content. Gel fractions of the resulting composite networks are high, ranging from 88%–100% and thermal stabilities do not vary significantly with composition. DMA and DSC analyses of the thiol-ene networks illustrate a tunable T_g which decreases with increasing C_{60} loading and is attributed to an increase in network free volume. A sub- T_g transition in the range of -90 to $-50\text{ }^{\circ}\text{C}$ is ascribed to local crankshaft motions in the methylene sections of the chains. The broadband dielectric spectrometer and the Keithley SCS measurements of the networks revealed higher ϵ' values as fullerene concentration increases. This was attributed to the increase in the concentration of the more polarizable network component and the freely rotating cage-surface hydroxyls. Along with increasing the dielectric permittivity, increasing the hydroxylated fullerene loading relative to other film constituents has led to a refining of the network structure as evidenced by a narrower glass transition and extremely high gel fraction for this composition. A general conclusion that can be drawn from these overall results is that this class of materials can be rendered quite polarizable, and the fact that ϵ' is considerably greater than ϵ'' suggests that they may prove useful as high-energy dielectric storage media for high capacitance applications.

Acknowledgments: J. Paige Buchanan gratefully acknowledges funding for this research provided through the National Science Foundation Early Career Development (CAREER) Program under award number CHE-0847481. Mohammad K. Hassan would like to acknowledge the Qatar University's financial support through the Center for Advanced Materials' Start-Up grant.

Author Contributions: All authors made critical contributions to the collection and interpretation of data and the writing of the final manuscript. Hanaa M. Ahmed (primary) and Amber D. Windham developed the synthetic strategies, prepared nanocomposite films, and collected physical data, including dielectric data, within the research labs and under the guidance of J. Paige Buchanan and Randy K. Buchanan. A more comprehensive dielectric analysis of nanocomposite films occurred under the direction of Kenneth A. Mauritz and Mohammad K. Hassan. Maryam M. Al-Ejji and Noora H. Al-Qahtani participated in the interpretation of the combined dielectric analysis data and in the construction of these manuscript sections. J. Paige Buchanan assembled the manuscript, combining the contributions from the coauthors.

Conflicts of Interest: The authors declare no conflict of interest.

References

1. Giacalone, F.; Martín, N. Fullerene polymers: synthesis and properties. *Chem. Rev.* **2006**, *106*, 5136–5190. [[CrossRef](#)] [[PubMed](#)]

2. Wang, C.; Guo, Z.-X.; Fu, S.; Wu, W.; Zhu, D. Polymers containing fullerene or carbon nanotube structures. *Prog. Polym. Sci.* **2004**, *29*, 1079–1141. [[CrossRef](#)]
3. McCluskey, D.M.; Smith, T.N.; Madasu, P.K.; Coumbe, C.E.; Mackey, M.A.; Fulmer, P.A.; Wynne, J.H.; Stevenson, S.; Phillips, J.P. Evidence for singlet-oxygen generation and biocidal activity in photoresponsive metallic nitride fullerene-polymer adhesive films. *ACS Appl. Mater. Interfaces* **2009**, *1*, 882–887. [[CrossRef](#)] [[PubMed](#)]
4. Kokubo, K.; Takahashi, R.; Kato, M.; Harada, A.; Noguchi, T.; Oshima, T. Thermal and thermo-oxidative stability of thermoplastic polymer nanocomposites with arylated [60]fullerene derivatives. *Polym. Compos.* **2014**. [[CrossRef](#)]
5. Hawker, C.J. A simple and versatile method for the synthesis of C60 copolymers. *Macromolecules* **1994**, *27*, 4836–4837. [[CrossRef](#)]
6. Badamshina, E.R.; Gafurova, M.P. Hydroxylated fullerenes and fullerene-containing poly(urethanes). *Polym. Sci. Ser. B* **2007**, *49*, 182–190. [[CrossRef](#)]
7. Ahmed, H.M.; Hassan, M.K.; Mauritz, K.A.; Bunkley, S.L.; Buchanan, R.K.; Buchanan, J.P. Dielectric properties of C60 and Sc3N@C80 fullerene containing polyurethane nanocomposites. *J. Appl. Polym. Sci.* **2014**, *131*. [[CrossRef](#)]
8. Lu, Z.; He, C.; Chung, T.S. Composites of multifunctional benzylaminofullerene with low-density polyethylene. *Polymer* **2001**, *42*, 5233–5237. [[CrossRef](#)]
9. Sudareva, N.N.; Saprykina, N.N.; Yudin, V.E. Comparison of bonds existing between C60 fullerene and polyamide molecules in various nanocomposite materials. *Fuller. Nanotub. Carbon Nanostruct.* **2015**, *23*, 807–817. [[CrossRef](#)]
10. Schönhals, A. Molecular Dynamics in Polymer Model Systems. In *Broadband Dielectric Spectroscopy*; Kremer, F., Schönhals, A., Eds.; Springer: Berlin/Heidelberg, Germany, 2003; pp. 225–293.
11. Schönhals, A.; Kremer, F. Analysis of Dielectric Spectra. In *Broadband Dielectric Spectroscopy*; Kremer, F., Schönhals, A., Eds.; Springer: Berlin/Heidelberg, Germany, 2003; pp. 59–98.
12. Hoyle, C.E.; Bowman, C.N. Thiol-ene click chemistry. *Angew. Chem. Int. Ed.* **2010**, *49*, 1540–1573. [[CrossRef](#)] [[PubMed](#)]
13. Hoyle, C.E.; Lowe, A.B.; Bowman, C.N. Thiol-click chemistry: A multifaceted toolbox for small molecule and polymer synthesis. *Chem. Soc. Rev.* **2010**, *39*, 1355–1387. [[CrossRef](#)] [[PubMed](#)]
14. Lowe, A.B. Thiol-ene “click” reactions and recent applications in polymer and materials synthesis. *Polym. Chem.* **2010**, *1*, 17–36. [[CrossRef](#)]
15. Tucker-Schwartz, A.K.; Farrell, R.A.; Garrell, R.L. Thiol-ene click reaction as a general route to functional trialkoxysilanes for surface coating applications. *J. Am. Chem. Soc.* **2011**, *133*, 11026–11029. [[CrossRef](#)] [[PubMed](#)]
16. Shin, J.; Nazarenko, S.; Phillips, J.P.; Hoyle, C.E. Physical and chemical modifications of thiol-ene networks to control activation energy of enthalpy relaxation. *Polymer* **2009**, *50*, 6281–6286. [[CrossRef](#)]
17. Fragiadakis, D.; Runt, J. Molecular dynamics of segmented polyurethane copolymers: influence of soft segment composition. *Macromolecules* **2013**, *46*, 4184–4190. [[CrossRef](#)]
18. Velankar, S.; Cooper, S.L. Microphase separation and rheological properties of polyurethane melts. 1. Effect of block length. *Macromolecules* **1998**, *31*, 9181–9192. [[CrossRef](#)]
19. Subocz, J.; Valozhyn, A.; Zenker, M. Effect of the carbon C60, C70 contents on the dielectric properties of polyimide films. *Rev. Adv. Mater. Sci.* **2007**, *14*, 193–196.
20. Ouyang, J.; Zhou, S.; Wang, F.; Goh, S.H. Structures and properties of supramolecular assembled fullerene/poly (dimethylsiloxane) nanocomposites. *J. Phys. Chem. B* **2004**, *108*, 5937–5943. [[CrossRef](#)]
21. Li, J.; Zhang, L.; Ducharme, S. Electric energy density of dielectric nanocomposites. *Appl. Phys. Lett.* **2007**, *90*. [[CrossRef](#)]
22. Doi, M.; Edwards, S.F. *The Theory of Polymer Dynamics*; Oxford University Press: New York, NY, USA, 1988, Volume 73.

